JOURNAL OF MAGNETIC RESONANCE **130,** 97–101 (1998)
ARTICLE NO. MN971286

3D C(CC)H TOCSY Experiment for Assigning Protons and Carbons in Uniformly ^{13}C- and Selectively ^{2}H-Labeled RNA

Kwaku T. Dayie, Thomas J. Tolbert, and James R. Williamson

Chemistry Department, Massachusetts Institute of Technology, 77 Massachusetts Avenue, Cambridge, Massachusetts 02139

E-mail: jrwill@mit.edu, kwaku@stentor.mit.edu.

Received May 20, 1997; revised September 8, 1997

We have prepared RNAs uniformly ^{13}C-labeled in the ribose ring and with the H3′, H4′, H5′/H5″ protons specifically replaced with deuterons (3′, 4′, 5′/5″-^{2}H–^{13}C, termed *d*4-^{13}C ribose), which offers the advantage of spectral simplification without sacrifice of sensitivity for the remaining protons. A 3D C(CC)H TOCSY experiment that uses a combination of cross-polarization transfer and deuterium decoupling improves the transfer of magnetization around the ribose ring and facilitates assignment of all ribose carbons and H1′ and H2′ protons in a 30-nucleotide RNA from HIV-2. These and other combinations of labeling and pulse sequence methodology should prove invaluable for the study of large RNAs, RNA–ligand, and RNA–protein complexes. © 1998 Academic Press

Key Words: **C(CC)H TOCSY; multidimensional NMR; HIV-2 TAR RNA; resonance assignment; deuteration.**

The investigation of RNA structures and RNA–ligand interactions has benefited from multidimensional heteronuclear NMR techniques that are facilitated by availability of isotopically labeled RNA (*1*). A plethora of triple-resonance experiments, analogous to those applied to proteins (*2*), have been adapted for labeled oligonucleotides (*3*). Using these experiments, the chemical shifts can be assigned for each nucleus in a polynucleotide chain for medium-sized RNAs. Because the ribose protons, carbons, and backbone phosphorous atoms resonate within a very narrow chemical shift range, complete assignment is very difficult for larger RNAs (>40 nucleotides). In addition, the rapid relaxation of these nuclei limits the application of many triple-resonance experiments that rely on small scalar couplings for magnetization transfer.

As part of our effort to extend the size limit of RNA structures that can be studied effectively by NMR, we have prepared specific isotopic-labeling patterns in RNAs and designed pulse sequences that take advantage of those patterns. We have prepared RNAs uniformly ^{13}C-labeled in the ribose ring and with the H3′, H4′, H5′/H5″ protons specifically replaced with deuterons (3′, 4′, 5′/5″-^{2}H–^{13}C, termed *d*4-^{13}C ribose), which offers the advantage of spectral simplification without sacrifice of sensitivity for the remaining protons. This deuteration pattern is a compromise between elimination of as many protons as possible while retaining as much structural information as possible. The remaining H1′ and H2′ scalar coupling affords the sugar pucker, the base to H1′ NOE affords the glycosidic torsion, and the exchangeable protons afford base pairing information, while other information on the backbone conformation is lost.

Uniformly ^{13}C- and *d*4-^{13}C ribose were prepared starting from ^{13}C-glucose (Cambridge Isotope Labs, Cambridge, MA) and ^{13}C–^{2}H glucose (Martek), respectively, using enzymes from the pentose phosphate pathway (Tolbert and Williamson, unpublished). The enzymatic ribose synthesis was directly coupled to nucleotide synthesis using a series of ribosyl transferases (*4*) to produce *d*4-^{13}C-ATP, -GTP, -UTP, and -CTP, with labeled sugars and unlabeled bases. As a test case, the 30-nucleotide hairpin loop from HIV-2 TAR RNA (5′ GGCCCAGAUUGACCUGGGAGCUCUC-UGGCC 3′) (*5*) was synthesized by *in vitro* transcription from a synthetic oligonucleotide template with T7 RNA polymerase (*6*) using the *d*4-^{13}C and ^{13}C NTPs. The RNA was purified as described previously (*4*) and dialyzed into 50 mM NaCl, 0.1 mM EDTA, 10 mM sodium phosphate, and exchanged into D_2O.

Substitution of deuterons for protons substantially reduces the directly attached carbon and proton linewidths and alleviates the resonance crowding in the ribose region. The labeling pattern where the H3′, H4′, and H5′/H5″ are substituted for deuterons simplifies the carbon HSQC spectrum (Fig. 1), since the H2′ resonances are the only protons in the region 4–5 ppm. As can be seen in Fig. 1B, all the C2′/H2′ resonances that are usually overlapped with the C3′/H3′ resonances are clearly observed in the spectra of the deuterated sample. A benefit of this labeling pattern is that the ribose carbons bearing deuterons will relax more slowly, and magnetization transfer through the sugar ring should be more efficient.

1090-7807/98 $25.00

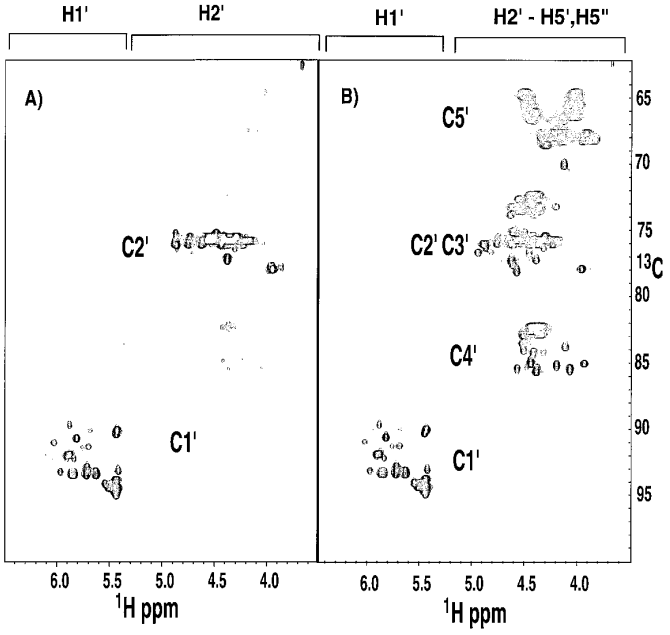

FIG. 1. An HSQC spectra of (A) 1.0 mM *d4*-^{13}C TAR from HIV-2 and (B) 1.1 mM ^{13}C TAR from HIV-2. Spectra were taken on the Varian Inova 600-MHz spectrometers using 32 scans/FID. Carbon and proton sweep widths were 6 kHz, and carriers were positioned at 81 ppm (^{13}C) and 4.8 ppm (^{1}H). Note how the overlap between the C2′ and C3′ resonances is removed in the deuterated sample.

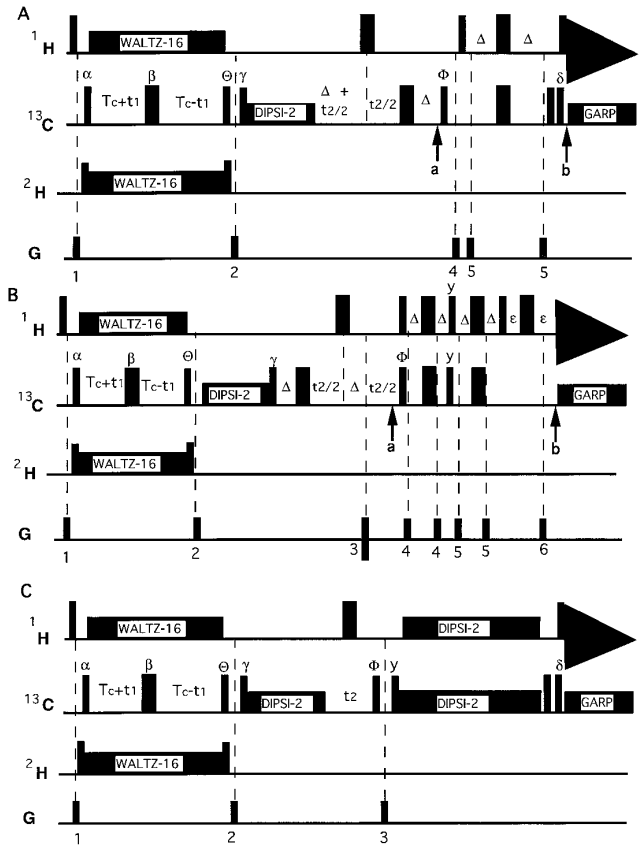

FIG. 2. Heteronuclear pulse sequences for (A) INEPT-based 3D constant time C(CC)H TOCSY, (B) INEPT-based 3D constant time C(CC)H TOCSY with sensitivity enhancement, and (C) CP-based 3D constant time C(CC)H TOCSY experiments. Thin and thick vertical bars represent 90° and 180° radiofrequency (RF) pulses respectively. ^{1}H, ^{2}H, and ^{13}C carriers are centered at 4.8 ppm, 3.0 ppm, and 81.0 ppm respectively. At high power, ^{1}H and ^{13}C RF pulses were applied using 27.4 and 23.1 kHz fields respectively. WALTZ-16 (*19*) decoupling at 6 kHz is applied on the ^{1}H channel to maintain the transverse carbon magnetization inphase during the constant time period, and during acquisition a 1.9-kHz field is applied to the carbon channel. For deuterium decoupling a 1-kHz field was employed, and the flanking 90° pulses were applied with a 2.5-kHz field. Three cycles of DIPSI-2 sequence yielding 13.0-ms isotropic TOCSY mixing time and one cycle of DIPSI-2 yielding a cross-polarization time of 6.1 ms were applied (For each new sample, it is advisable to run half-hour 2D versions of the pulse sequence to determine empirically the optimal TOCSY mixing time in the theoretical range 6–24 ms (*18*)). The TOCSY field strength was at 6.6 kHz, whereas the cross-polarization field was at 4.7 kHz. The delay Δ was set to slightly less than $\frac{1}{4}\,J_{CH}$ at 1.5 ms, and T_C to 12.5 ms. Nonlabeled pulses are applied along the *x* axis. For (A and C), quadrature in F_2 and F_3 were achieved by incrementing the phases of α, γ, and the DIPSI-2 TOCSY in States–TPPI fashion. All gradients are applied for about 500 μs at 0.05–0.10 T m^{-1}. For (B), two FIDs are acquired for each increment of t_2 with the amplitude of G_3 and the phase Φ inverted in the second FID. The gradients G_3 and G_6 are used for coherence selection: their durations and strengths are G_3, 1.6 ms, 0.15 T m^{-1}; G_6, 0.4 ms, 0.15 T m^{-1} (it is necessary to fine tune the G_6 gradient strength relative a fixed value of G_3 in order to obtain the requisite proton and carbon gyromagnetic ratios, γ_H and γ_C). To implement (A and B) using WATERGATE (*15*) for water suppression simply replace the portions marked between the two arrows delineated by a and b, asshown for example in Ref. (*20*).

Pulse sequences designed to exploit this property are shown in Fig. 2. These experiments are similar in spirit to the C(CC)(CO)NH experiment developed for use in deuterated proteins (*7*). The experiments begin with the creation of transverse carbon magnetization which is frequency labeled in a constant-time fashion (*8*), followed by its transfer through the ribose ring using DIPSI-2 TOCSY (*9*) sequence, and finally detected on the remaining H1′/H2′ protons. The flow of magnetization is shown below:

$$^{13}\mathrm{C}(t_1) \xrightarrow{J_{CC}} \xrightarrow{J_{CH}} \mathrm{H}(t_3) \quad \text{2D C(CC)H TOCSY}$$

$$^{13}\mathrm{C}(t_1) \xrightarrow{J_{CC}} {}^{13}\mathrm{C}(t_2) \xrightarrow{J_{CH}} \mathrm{H}(t_3) \quad \text{3D C(CC)H TOCSY.}$$

The couplings involved in each transfer step are shown above the arrows, and t_1–t_3 represent the acquisition times. In the design of the pulse sequences, the transfer of magnetization from the deuterated carbons to the protonated carbons was optimized using a combination of constant-time (*8*), cross-polarization transfers (*10*), and deuterium decoupling (*11*). Pulsed field gradients are used to minimize artifacts and reduce any trace of residual water in the spectra. Cross-polarization efficiently transfers magnetization from the carbons to the directly attached protons (Fig. 3) as demon-

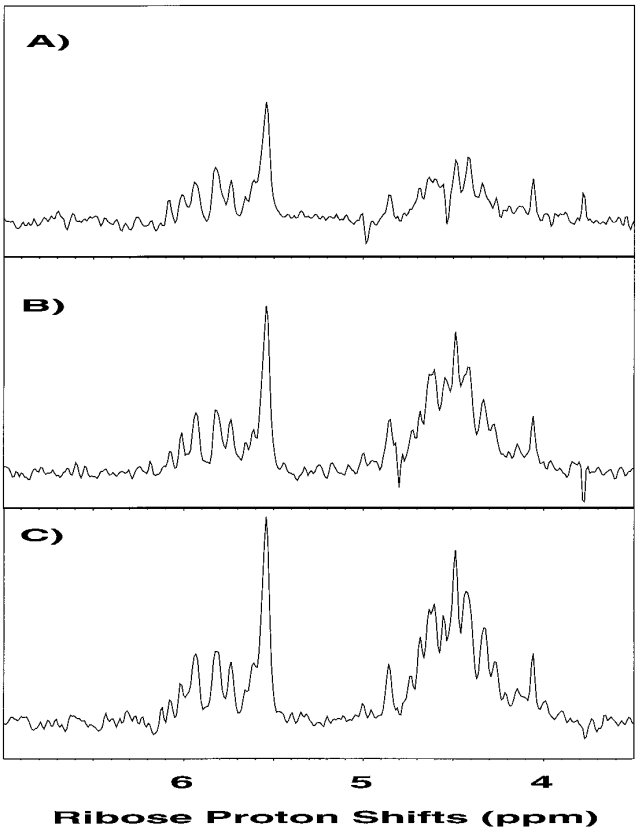

FIG. 3. One-dimensional spectra of CT-C(CC)H TOCSY spectra of *d4*-^{13}C TAR using (A) C → H CP transfer without deuterium decoupling, (B) C → H INEPT transfer with deuterium decoupling, and (C) C → H CP transfer with deuterium decoupling. Spectra were taken on the Varian Inova 600-MHz spectrometer.

strated by a number of workers (*12*); deuterium decoupling as expected improves the signal-to-noise considerably (Fig. 3). The pulses can also be implemented with the preservation of the two orthogonal coherence pathways (*13*) combined with gradients to select the desired coherence pathway (*14*) (Fig. 2B) or with WATERGATE water suppression scheme (*15*) for samples in water. In our hands we do not observe any significant gain with the gradient, sensitivity-enhanced versions. Use of constant time improves the resolution in the carbon dimension by eliminating the ^{13}C homonuclear coupling, and allows one to distinguish the 1′ and 5′ resonances from the 2′, 3′, and 4′ resonances, since ambiguities occasionally arise for nucleotides with unusual chemical shifts (*16*). Finally, by beginning the experiment with carbon magnetization, even the deuterated carbons can be assigned and the length of the pulse sequence is reduced.

In current protocols for identifying the sugar proton and carbon spin systems, one typically records several 3D experiments such as HCCH-COSY, HCCH-RELAY, and HCCH-TOCSY to connect the ribose and carbon resonances to the relatively well-resolved H1′/C1′ region (*17*). For larger RNA molecules, magnetization transfer around the sugar ring becomes inefficient, especially for the C4′ and C5′ resonances due to rapid carbon relaxation. The ribose carbons (C1′–C5′) in uniformly ^{13}C-labeled RNA approximate a linear five-spin coupling network found in lysine residues, and the optimal isotropic mixing times (12.5–25 ms) for transfer through the chain have been calculated (*18*). In practice for the *d4*-^{13}C sample and the new pulse scheme, we find that a 13-ms TOCSY mixing time is optimal for the observation of the entire ribose spin system simultaneously. Other mixing times (6–24 ms) optimize magnetization transfer between a subset of the ribose carbons. In comparison, this transfer is incomplete for the ^{13}C-only sample (Fig. 4A). While it is more difficult to deconvolute the connectivity pattern in the 2′ region using a fully protonated sample, in the deuterated sample we obtain parallel ladders of carbon resonances at the chemical shift of each H1′ and H2′ pair, which provide two independent routes for assigning the carbon resonances. An example of this ladder is shown for G32 in Fig. 4 (obtained with the pulse sequence in Fig. 2C). One surprising observation is that crosspeaks are better dispersed in the H2′/C1′ region than in the H1′/C1′ region. This is clearly seen in Fig. 4B for G32 and G33 whose overlapped resonances in the H1′ position are well resolved

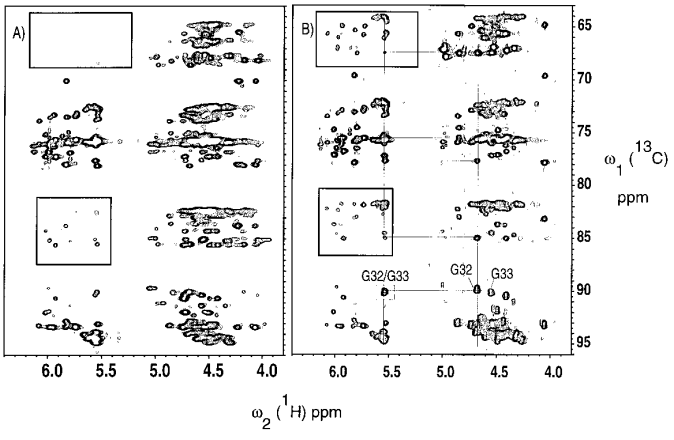

FIG. 4. Two-dimensional CT-C(CC)H TOCSY spectra of (A) ^{13}C only TAR and (B) *d4*-^{13}C TAR at 25°C using the sequence in Fig. 2C. Spectra were recorded on a Varian Inova 600-MHz spectrometer using 16 scans per increment. The parallel ladder of carbon resonances at the chemical shifts of the H1′ and H2′ are shown for G32.

The phase cycle for (A and C) is as follows: $\alpha = x$; $\beta = x, y, -x, -y$; $\delta = [8x, 8(-x)]$; $\theta = [2x, 2(-x)]$; $\Phi = [4y, 4(-y)]$; $\gamma = y$, and rec $= [(x, -x, -x, x), (-x, x, x, -x)]$. For (B) the phase cycle is $\gamma = [4y, 4(-y)]$, and $\Phi = x$; all the other phases are the same as those for (A and C). The pulse program is available from the authors (kwaku@stentor.mit.edu).

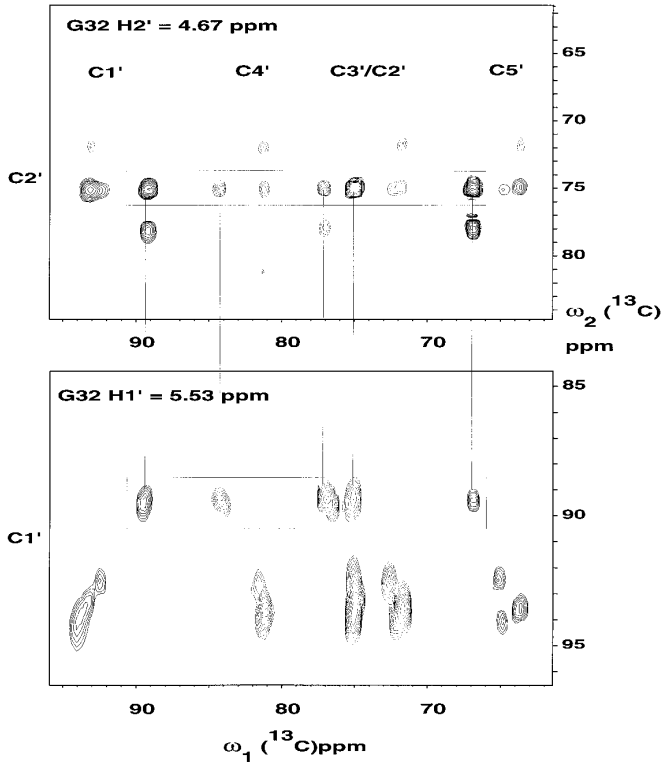

FIG. 5. Carbon–carbon planes at particular proton frequencies from 3D CT-C(CC)H TOCSY spectra of *d4*-^{13}C TAR at 25°C using the sequence in Fig. 2C. Spectra were recorded on a Varian Inova 600-MHz spectrometer using 16 scans per increment, with a recycle delay of 2.5 s, and a 64 × 24 × 512 complex data set, resulting in a total acquisition time of 75 h. Slices are shown for G32 at H2′ (4.67 ppm) and H1′ (5.53 ppm) planes. The crowded region at 5.53 ppm in Fig. 4 is easily resolved in the 3D using planes at both H1′ and H2′ chemical shifts. The recycle delay was determined empirically by recording 1D spectra as function of delay time to give 80% of the maximum signal. The nonselective relaxation times T_1 ($^{13}C_D$, $^{13}C_H$) (in seconds) determined for both samples by 1D saturation recovery were C1′ (1.26, 0.93), C2′ (1.0, 0.78), C3′ (0.95, 2.63), C4′ (1.04, 2.2), and C5′ (0.53, 2.58).

in the H2′ position. Finally, at a lower temperature of 5°C (which approximates the effect of an RNA 1.6 times bigger than TAR), the transfer through the sugar ring spin system is inferior for the ^{13}C-only sample compared to that in the *d4*-^{13}C sample where magnetization is relayed completely from the 5′ to 1′ region for most resonances (data not shown).

For small molecules one can in principle assign all the carbon resonances in a 2D experiment. For larger RNAs with extensively overlapped peaks, a dispersion into the third dimension can simplify the analysis. Two representative planes from a constant time 3D C(CC)H TOCSY experiment using the pulse sequence in Fig. 2C are shown in Fig. 5. The parallel ladder of carbon crosspeaks in the corresponding H1′ and H2′ planes serves as an internal consistency check of the assignments at the H1′ and H2′ positions (Fig. 5). As can be seen from Fig. 5 all the carbon resonances are easily assigned at the C1′ and C2′ chemical shifts in the carbon–carbon plane at each H1′ or H2′ resonance position. An example is shown for G32 at both the H1′ and H2′ planes. Note how the overlap of the G32 with G33 in the H1′ position is easily resolved in the H2′ plane. The use of a constant-time delay proportional to an odd integer multiple of the one-bond carbon–carbon scalar coupling constant ($1/J_{CC}$) allows one to easily distinguish 1′ and 5′ resonances from the 2′, 3′, and 4′ resonances because in this case the sign of the cross peaks for C1′ and C5′ resonances is opposite to that of C2′, C3′, and C4′ resonances.

In summary, new isotopic-labeling patterns and NMR experiments are presented that facilitate assignment of all ribose carbons and H1′ and H2′ protons in RNAs uniformly ^{13}C-labeled and selectively deuterated at the 3′, 4′, 5′, and 5″ positions. The combination of selective deuteration, cross-polarization transfer, and deuterium decoupling improves the transfer of magnetization around the ribose ring. These and other combinations of labeling and pulse sequence methodology should prove invaluable for the study of large RNAs, RNA–ligand, and RNA–protein complexes.

ACKNOWLEDGMENTS

This work was supported by the Alfred P. Sloan Foundation, the National Institutes of Health (GM-53757), and the Jane Coffin Childs Memorial Fund for Medical Research (K.T.D.).

REFERENCES

1. (*a*) R. T. Batey, M. Inada, E. Kujawinski, J. D. Puglisi, and J. R. Williamson, *Nucl. Acid Res.* **20,** 4515–4523 (1992); (*b*) E. P. Nikonowicz, A. Sirr, P. Legault, F. M. Jucker, L. M. Baer, and A. Pardi, *Nucl. Acid Res.* **20,** 4507–4513 (1992); (*c*) M. J. Michnicka, J. W. Harper, and G. C. King, *Biochemistry* **32,** 395–400 (1993).
2. (*a*) A. Bax and S. Grzesiek, *Acc. Chem. Res.* **26,** 131–138 (1993); (*b*) G. M. Clore and A. M. Gronenborn, *Methods Enzymol.* **239,** 349–363 (1994).
3. (*a*) T. Dieckmann and J. Feigon, *Curr. Opin. Struct. Biol.* **4,** 745–749 (1994); (*b*) A. Pardi, *Methods Enzymol.* **261,** 350–380 (1995); (*c*) G. Varani, F. Aboul-ela, and FH. T. Allain, *Prog. NMR Spectrosc.* **29,** 51–127 (1996).
4. T. J. Tolbert and J. R. Williamson, *J. Am. Chem. Soc.* **118,** 7929–7940 (1996).
5. A. S. Brodsky and J. R. Williamson, *J. Mol. Biol.* **267,** 624–639 (1997).
6. J. F. Milligan and O. C. Uhlenbeck, *Methods Enzymol.* **180,** 51–62 (1987).
7. B. T. Farmer, II and R. A. Venters, *J. Am. Chem. Soc.* **117,** 4187–4188 (1995).
8. (*a*) J. Santoro and G. C. King, *J. Magn. Reson.* **97,** 202–207 (1992); (*b*) F. J. M. van de Ven and M. E. P. Philippens, *J. Magn. Reson.* **97,** 637–644 (1992); (*c*) G. W. Vuister and A. Bax, *J. Magn. Reson.* **98,** 428–435 (1992).

9. A. J. Shaka, C. J. Lee, and A. Pines, *J. Magn. Reson.* **77,** 274–293 (1988).

10. (*a*) R. D. Bertrand, W. B. Moniz, A. N. Garroway, and G. C. Chingas, *J. Am. Chem. Soc.* **100,** 5227–5229 (1978); (*b*) L. Müller and R. R. Ernst, *Mol. Phys.* **38,** 963–992 (1979); (*c*) A. Majumdar and E. R. P. Zuiderweg, *J. Magn. Reson. A* **113,** 19–31 (1995); (*d*) V. V. Krishnan and M. Rance, *J. Magn. Reson. A* **116,** 97–106 (1995).

11. (*a*) S. Grzesiek, J. Anglister, H. Ren, and A. Bax, *J. Am. Chem. Soc.* **115,** 4369–4370 (1993); (*b*) D. M. Kushlan and D. M. LeMaster, *J. Biomol. NMR* **3,** 701–708 (1993).

12. (*a*) A. Majumdar, H. Wang, R. C. Morshauser, and E. R. P. Zuiderweg, *J. Biomol. NMR* **3,** 387–397 (1993); (*b*) H. Wang and E. R. P. Zuiderweg, *J. Biomol. NMR* **5,** 207–211 (1995); (*c*) M. Sattler, P. Schimdt, J. Schleucher, O. Schedletzky, S. J. Glaser, and C. Griesinger, *J. Magn. Reson. B* **108,** 235–242 (1995); (*d*) M. Sattler, M. G. Schwendinger, J. Schleucher, and C. Griesinger, *J. Biomol. NMR* **6,** 11–22 (1995); (*e*) S. S. Wijmenga, E. Steensma, and C. P. M. van Mierlo, *J. Magn. Reson.* **124,** 459–467 (1997).

13. J. Cavanagh, A. G. Palmer III, P. E. Wright, and M. Rance, *J. Magn. Reson.* **91,** 429–436 (1991).

14. L. E. Kay, P. Keifer, and T. Saarinen, *J. Am. Chem. Soc.* **114,** 10,663–10,665 (1992).

15. V. Sklenar, M. Piotto, R. Leppik, and V. Saudek, *J. Magn. Reson. A* **102,** 241–245 (1993).

16. (*a*) J. L. Battiste, R. Tan, A. D. Frankel, and J. R. Williamson, *J. Biomol. NMR* **6,** 375–389 (1995); (*b*) T. Dieckmann and J. Feigon, *J. Biomol. NMR* **9,** 259–272 (1997).

17. (*a*) A. Pardi and E. P. Nikonowicz, *J. Am. Chem. Soc.* **114,** 9202–9203 (1992); (*b*) E. P. Nikonowicz and A. Pardi, *J. Mol. Biol.* **232,** 1141–1156 (1993).

18. (*a*) H. L. Eaton, S. W. Fesik, S. J. Glaser, and G. P. Drobny, *J. Magn. Reson.* **90,** 452–463 (1990); (*b*) S. J. Glaser, H. Schwalbe, J. P. Marino, and C. Griesinger, *J. Magn. Reson. B* **112,** 160–180 (1996).

19. A. J. Shaka, J. Keeler, T. Frenkiel, and R. Freeman, *J. Magn. Reson.* **52,** 335–338 (1983).

20. K. T. Dayie and G. Wagner, *J. Am. Chem. Soc.* **119,** 7797–7806 (1997).